Robust stochastic optimization for reservoir operation

Limeng Pan[1], Mashor Housh[2,3], Pan Liu[4], Ximing Cai[2], and Xin Chen[1]

[1]Department of Industrial and Enterprise Systems Engineering, University of Illinois, Urbana, Illinois, USA, [2]Department of Civil and Environmental Engineering, University of Illinois, Urbana, Illinois, USA, [3]Faculty of Management, Department of Natural Resources and Environmental Management, University of Haifa, Israel, [4]The State Key Laboratory of Water Resources and Hydropower Engineering Science, Wuhan University, Wuhan, Hubei, China

Abstract Optimal reservoir operation under uncertainty is a challenging engineering problem. Application of classic stochastic optimization methods to large-scale problems is limited due to computational difficulty. Moreover, classic stochastic methods assume that the estimated distribution function or the sample inflow data accurately represents the true probability distribution, which may be invalid and the performance of the algorithms may be undermined. In this study, we introduce a robust optimization (RO) approach, Iterative Linear Decision Rule (ILDR), so as to provide a tractable approximation for a multiperiod hydropower generation problem. The proposed approach extends the existing LDR method by accommodating nonlinear objective functions. It also provides users with the flexibility of choosing the accuracy of ILDR approximations by assigning a desired number of piecewise linear segments to each uncertainty. The performance of the ILDR is compared with benchmark policies including the sampling stochastic dynamic programming (SSDP) policy derived from historical data. The ILDR solves both the single and multireservoir systems efficiently. The single reservoir case study results show that the RO method is as good as SSDP when implemented on the original historical inflows and it outperforms SSDP policy when tested on generated inflows with the same mean and covariance matrix as those in history. For the multireservoir case study, which considers water supply in addition to power generation, numerical results show that the proposed approach performs as well as in the single reservoir case study in terms of optimal value and distributional robustness.

1. Introduction

Reservoirs are built to regulate variable water inflows for water uses (e.g., water supply and hydropower generation) and flooding control. Unfortunately, many reservoirs fail to provide the level of economic benefits to justify their high investment [*World Commission on Dams*, 2000] due to various factors and obstacles. Some are from institutional restrictions, for example, the safety and environmental regulations (as identified by *Oliveira and Loucks* [1997]), which are beyond the scope of this paper. *Labadie* [2004] characterizes the difficulties in optimizing large-scale reservoir operation problems as "high-dimensional, dynamic, nonlinear, and stochastic." The reservoir operation optimization problem is "among the most intractable classes in numerical computation" [*Escudero*, 2000]. These difficult problems have been studied by various methods. Early approaches include stochastic dynamic programming (SDP) [*Stedinger et al.*, 1984] and chance-constrained linear programming [*ReVelle et al.*, 1969; *Takeuchi*, 1986], as reviewed in *Yeh* [1985]. *Bhaskar and Whitlatch* [1987] conclude that the policies from SDP achieve lower average annual losses while maintaining equal or higher reliability levels when compared to policies derived from chance-constrained linear programming methods.

While SDP is designed to solve dynamic and stochastic problems and to be flexible with nonlinear objective functions, it requires full distributional information, i.e., the PDF of reservoir inflows. To avoid estimating the probability density function (PDF) explicitly, sampling stochastic dynamic programming (SSDP) was introduced to the reservoir management literature by *Kelman et al.* [1990], which uses the sample time series directly to construct the transition probability. However, both SDP and SSDP suffer from the "curse of dimensionality" [*Labadie*, 2004]. To build the transition probability matrix, it usually requires statistical models with long lag correlations. This is because inflows from the current time period are correlated with inflows from the previous "lag" time periods and the consideration of the correlation is necessary in

stochastic reservoir operation studies, for instance, studying the effect of droughts. To incorporate the long lag correlation, a high order (e.g., autoregressive models with many autoregressive terms) is needed, which leads to high-dimensional state space in SDP and causes a heavy computational burden. Moreover, both SDP and SSDP approaches require the discretization of state space. Reservoir operation optimization problems usually have a long planning horizon to include the entire seasonal cycle. Suppose the inflow and each state variable are discretized into d segments and the planning horizon is T, the objective function would be evaluated $O(Td^{lag+1})$ times in SDP and SSDP.

Many studies tried to tackle the "curse of dimensionality." To list a few, *Trezos and Yeh* [1987] propose a stochastic differential dynamic programming approach to maximize the electricity production without discretizing the state space to avoid the "curse of dimensionality"; *Cervellera et al.* [2006] propose an approach based on efficient discretization of the state space and approximation of the value functions over the continuous state space by means of a flexible feed-forward neural network. *Tilmant et al.* [2008] propose a sampled hyperplane, which suggests an outer approximation to the benefit-to-go function. However, all these methods heavily depend on the accuracy of the uncertainty distribution assumption. This paper proposes a new method, which does not rely on the full knowledge of PDF and attempts to address computational difficulties for reservoir operation optimization problems with uncertain inflows and nonlinear objective functions.

To tackle the "curse of dimensionality," avoid the risk of arbitrary assumption on the uncertainty distribution function, and maintain the capability for accurately maximizing concave nonlinear objective functions, distributionally robust Iterative Linear Decision Rule (ILDR) is proposed in this paper. With ILDR, every decision variable is modeled by a linear function (LDR) of the hydrologic variables. One example of an LDR for release at time t can be written as $r_t = r_t^0 + \sum_{k=1}^{t-1} r_t^k q_k$ where $q_k, k \leq t-1$ are the inflows that have been observed; $r_t^k, k = 0, 1, \ldots, t-1$ are the coefficients that will be determined by solving the optimization problem. With LDR, the observed realizations of the uncertain inputs are dynamically adopted in linear decision rules, and thus new information revealed from the uncertain process is utilized to achieve a good performance. The LDR leads to a Second-Order Cone Problem (SOCP), which is tractable and can be efficiently solved by interior point methods. The existing LDR approach in RO literature requires a piecewise linear objective and linear constraints [*Ben-Tal et al.*, 2009]. ILDR is designed to solve problems with nonlinear objective functions. The case studies show that problems with concave nonlinear objectives can be successfully solved. Since only the bounds, mean, and the covariance of the inflows are needed in the ILDR formulation, the proposed method is immunized against inaccurate PDF assumptions required by SDP. Compared to SSDP, ILDR does not need to construct a transition probability matrix and thus it is not heavily dependent on time series data. Thus when the test data set is different from the sample data set, ILDR may outperform SSDP.

The proposed ILDR method is closely related to the nonprobabilistic RO literature. RO can be classified into two categories, probabilistic RO [*Mulvey et al.*, 1995] and nonprobabilistic RO [*Ben-Tal et al.*, 2009]. The former quantifies uncertainty by probability distribution functions and the latter seeks an optimal solution that is feasible for any realization of the uncertainty (within bounds) and optimizes the worst case scenario. Although nonprobabilistic RO immunizes the solution very well, it can be too conservative. To overcome this drawback, *Ben-Tal et al.* [2004] introduce the *Adjustable Robust Counterpart* (ARC), to model the decisions that are made after decision makers observe the uncertainties in previous time periods. These decisions are called recourse decisions. In general, the ARC is not tractable; however, a tractable formulation is obtained when the recourse decisions are modeled as a linear function of the uncertainties, i.e., *Affinely Adjustable Robust Counterpart* (AARC). The decision variable in AARC is modeled by LDR. To capture the asymmetry of the uncertainty distribution, *Chen et al.* [2007] define forward and backward deviations and use them to derive better approximations of chance constraints. To further improve the performance, *Chen et al.* [2008] propose Deflected Linear Decision Rule (DLDR). *Chen and Zhang* [2009] propose *Extended Affinely Adjustable Robust Counterpart* (EAARC), where the decision variables are modeled as piecewise linear functions of the uncertain inputs (e.g., streamflows). The essential idea of these approaches is to model and incorporate the distributional information while maintaining the tractability.

It is necessary to notice that the ILDR method in this study is different from the well-known scenario-based RO, which belongs to probabilistic RO. One recent application provided by *Escudero* [2000] solved a multi-period reservoir planning problem, based on a multistage scenario tree, in which a solution is obtained for

each scenario. Although a solution is generated for each scenario, the second-stage solutions are not implementable since the actual occurrence may differ from any of the assumed scenarios. Similar to SDP, this scenario-based RO also requires the assumption of the uncertainty distribution and thus it is subject to the risk of inaccurate PDF assumption. Another disadvantage of scenario-based RO is the potential loss of tractability. As pointed out by *Watkins and McKinney* [1997], "One disadvantage of RO is the potential size and complexity of the resulting model. As a result, special solution algorithms may be required."

It is also necessary to mention that the ILDR presented in this study is different from the traditional LDR in reservoir management literature, as introduced by *ReVelle et al*. [1969]. First, in *ReVelle et al*. [1969], the rules are linear functions of the state variables while in this study the LDR is a function of the uncertainties. Second, our method utilizes the distributional information of the uncertainty, such as the support (The support of an uncertainty is the smallest closed set whose complement has zero probability.), mean and covariance matrix, which can be easily obtained from the historical data, while the traditional LDR may not be able to include information on the distributions of uncertain parameters; even when they are able to, they require a complete specification of the distribution. Third, the proposed formulation ends up with a tractable conic optimization problem instead of a linear programming problem as in the traditional LDR. Fourth, as an extension of LDR, we generalize the LDR as a piecewise linear functions of the uncertainties.

This is not the first study of reservoir operations by nonprobabilistic RO. *Housh et al*. [2012] apply the static version of the nonprobabilistic RO within a folding horizon framework to a multiyear management of water supply system. Folding horizon is a concept in multiple periods optimization. The optimal policy is derived for all the periods in the planning horizon but only the first one (few) period(s) in the optimal policy is implemented. A new optimization is conducted at the end of the last period that has been implemented; the second implementation follows the second optimization, and so forth. However, to the best of our knowledge, this work represents the first study of reservoir operation by adjustable nonprobabilistic RO. Moreover, the proposed ILDR method is an extension to the existing adjustable nonprobabilistic RO literature because it allows nonlinear objective functions.

Parameterization-Simulation-Optimization (PSO) [*Koutsoyiannis and Economou*, 2003] is another parameterized rule method for reservoir management. Unlike LDR approaches, which parameterizes decisions into linear or piecewise linear functions of realized uncertainties, PSO can parameterize them into any general functions, which are usually functions of the state variables. It uses sample paths to simulate the system with the parameterized decision rules. The simulation output forms an optimization problem of the parameters, which is then solved by some proper optimization methods. The PSO approach has some advantages over the proposed method. First, because it does not require linearity of the objective functions, state transition equations, or the constraints, it can be applied to more general problems. Second, it can be easily extended to multiobjective problems, for example, through evolutionary algorithms [*Pianosi et al*., 2011]. Finally, by proper choices of the decision rules, it can be viewed as an improvement of the management system, which increases its acceptability to actual decision makers [*Oliveira and Loucks*, 1997]. However, as all simulation or scenario-based approaches, PSO requires a large data set to make the simulation meaningful. PSO usually provides an approximate solution to the optimization problem, while the proposed method gives a nearly exact one. Thus, there is a trade-off between having an approximate solution to a more general problem (PSO) or an exact solution to a more restricted problem (ILDR). In section 5, potential improvements are suggested to extend the proposed method to more general problems.

In summary, the proposed method is preferred when the objective is concave in a maximization problem (convex in a minimization problem), the constraints are linear, and all the four difficulties (high-dimensional, dynamic, nonlinear, and stochastic) exist in the problem; especially when the distribution of the inflows is unknown or the inflows are correlated with long lag or the scale of the problem is large. Two case studies are provided to illustrate the advantage of the proposed method. One is a single reservoir study on the Three Gorges Reservoir (TGR) in China. As a single reservoir problem with a nonlinear objective function, it can be solved by SSDP. The proposed method performs as well as SSDP when tested with historical inflows and outperforms SSDP when they are simulated with generated inflows. The PDF of the generated inflows is different from the recorded historical data but still maintains the same mean and covariance matrix. The proposed method is only compared with SSDP because SSDP can properly utilize the limited historical data to estimate the probability transition matrix and accommodate nonlinear objective functions. Comparing with SSDP, SDP requires a perfect foresight of the multivariable distribution of

the water inflows [*Kelman et al.*, 1990] which requires larger data sets than the one available. The second study is a multiple-reservoir case from the Central Valley Project system (CVP) in the United States. In this case study, since SSDP is no longer applicable due to computational time and computer memory limitations, the objective value from a deterministic optimization problem, OP, is used as the benchmark. In OP, all the future inflows are revealed. Thus the objective value of OP represents the highest that could possibly be obtained. Our proposed method achieves more than 95% of that of OP in the multireservoir case study.

The remaining of this paper is organized as follows. Section 2 introduces the reservoir optimization problem. Section 3 uses hydro-power generation maximization problem to introduce the ILDR method. In section 4, the ILDR approach is tested with two case studies. Throughout the paper, bold lower case letters denote vectors and upper case letters represent matrices. For a general variable x, $\bar{x}$ and $\underline{x}$ denote the upper and lower bounds of x, respectively; $\hat{x}$ represents the expected value of x.

2. Reservoir Optimization Problem

For simplicity, a single reservoir optimization problem is used to introduce our approach, which is then applied on a multireservoir system. The reservoir starts with s_1 representing the storage. T releases will be made throughout the planning horizon, which is divided into T time periods with exactly one release in one period. During time period t, the amount of inflow is a random variable q_t whose value is not revealed until the beginning of time period $t-f+1$. Here $f \geq 0$ is the number of periods into the future that can be accurately forecasted. $f = 0$ means there is no forecast. At the beginning of time period t, a release r_t is decided based on the available information. This information includes the realized and forecasted inflows $q_1, q_2, \ldots, q_{t-1+f}$ and the storage volumes $s_1, \ldots, s_t$. Thus r_t can be viewed as a function that maps the available information to a release in the amount of r_t. Here the function name and its value are both denoted by r_t to keep the notations in the paper concise. r_t is restricted by a maximum and minimum bound release, $\underline{r}_t \leq r_t \leq \bar{r}_t$. During period t, an economical benefit of $b_t(r_t, s_t)$ is generated. Here b_t is a function of s_t and r_t. The goal is to maximize the sum of expected benefits in all periods:

$$E_{\mathbf{q}}\left[\sum_{t=1}^{T} b_t(r_t, s_t) + b_{T+1}(s_{T+1})\right],$$

where $b_{T+1}(s_{T+1})$ is the terminal condition that prevents the optimization from leaving only the minimum required water ($\underline{s}_{T+1}$) at the end of the planning horizon.

To summarize, the multiperiod stochastic optimization problem for reservoir operations can be formulated as

$$\max_{\mathbf{r}} E_{\mathbf{q}}\left[\sum_{t=1}^{T} b_t(r_t, s_t) + b_{T+1}(s_{T+1})\right] \tag{1a}$$

$$s.t. \quad s_{t+1} = s_t + q_t - r_t, \tag{1b}$$

$$\underline{r}_t \leq r_t \leq \bar{r}_t, \quad t = 1, 2, \ldots, T, \tag{1c}$$

$$\underline{s}_t \leq s_t \leq \bar{s}_t, \quad t = 1, 2, \ldots, T+1, \tag{1d}$$

where constraint (1d) is based on regulations for safety, floods, and drought control; $\mathbf{r}$ is a policy consisting of T releasing decisions $\mathbf{r} \triangleq [r_1, r_2, \ldots, r_T]'$. Each of its components, r_t, is a function of the information that is available when r_t is decided. This functional relationship can be described in greater details using the state transition equation (1b). At the beginning of period 1, the optimal release depends on s_1. If $f \geq 1$, r_1 also depends on $q_1, \ldots, q_f$. Based on (1b), one can recursively find that both r_t and s_t are determined by s_1 and $q_1, \ldots, q_{t-1+f}$.

To simplify the notation, define $q_0 = s_1$ and the hydrologic information available to the decision maker at the beginning of period t, denoted by $\mathbf{q}_t$, can be written as

$$\mathbf{q}_t \triangleq [q_0, q_1, q_2, \ldots, q_{t-1+f}]'. \tag{2}$$

Thus

$$r_t \triangleq r_t(\mathbf{q}_t), \tag{3}$$
$$s_t \triangleq s_t(\mathbf{q}_t). \tag{4}$$

Dyer and Stougie [2006] show that the model represented by (1) is at least ♯P-hard even when the exact distribution is known and the benefit function is linear. Here ♯P-hard is another concept in computational complexity to identify a class of problems that are even more challenging than NP-complete problems. In addition, as indicated by *Labadie* [2004], the benefit function $b_t(\cdot)$ can be highly nonlinear especially for the case of maximizing hydro-power generation.

Because of the uncertainties and the fact that the policy is a vector of functions, problem (1) has infinite dimension. But if we restrict (3) to be linear on $\mathbf{q}_t$, it becomes a linear decision rule (LDR). Because of the linearity of state transition equation and (4), s_t will also be an LDR. This restriction reduces the dimension of decisions' functional space from infinite to finite. The optimization reduces to search for the optimal coefficients of $\mathbf{q}_t$ for r_t. This leads to a tractable Second-Order Cone Problem (SOCP) as to be shown in section 3.3.

3. Distributionally Robust Iterative Linear Decision Rule Approach

Although formulating the problem by LDR utilizes the linearity of the state transition equation and leads to a tractable optimization problem, it requires the objective function to be linear. In this section, we introduce an iterative LDR (ILDR) approach, which solves problems with nonlinear objective functions such as the reservoir operation problems considered herein. A hydro-power generation planning problem is chosen to illustrate how ILDR solves a high-dimensional, nonlinear, dynamic, and stochastic problem of reservoir operation.

Hydro-power Generation Problem: The dam blocks water in the reservoir to reach a certain height above the turbine. This height creates water head which is used to turn the turbines of the power plants. The larger the head and the faster water flows through the turbines, the more energy is generated. This energy corresponds to the benefit in the optimization problem. In time period t, it is

$$b_t = \min(h_t, b_t^{max}), \tag{5}$$

where

$$h_t = K(r_t - \underline{r}_t)(z_t - e_t). \tag{6}$$

In (6), K is a constant coefficient depicting generating efficiency and unit conversion; z_t is the reservoir water elevation determined by s_t; e_t is the tail water elevation and a function of r_t; b_t^{max} is the per period maximum output under equipped turbines. $\underline{r}_t$ is subtracted from r_t because $\underline{r}_t$ includes releases from navigation locks and evaporation and does not end with power generation. Both h_t and b_t are functions of r_t and s_t:

$$h_t = h_t(r_t, s_t),$$
$$b_t = b_t(r_t, s_t).$$

These nonlinear relations vary for different reservoirs. Analysis of the hydrographic data shows that the elevation-storage curve for the Three Gorges Reservoir could be estimated as a quadratic function:

$$z_t(s_t) \approx -0.017s_t^2 + 2.359s_t + 109.529, \tag{7}$$

and e_t follows a linear function of r_t:

$$e_t(r_t) \approx 0.022r_t + 62.870. \tag{8}$$

With (7) and (8) plugged into (6), we can explicitly write b_t as a nonlinear function of r_t and s_t. In terms of $b_{T+1}(s_{T+1})$, the potential benefit from the terminal water storage s_{T+1}, its value depends on how the water is managed in the future. We assume the next cycle will be planned by a similar optimization, and a valid estimation would be:

$$b_{T+1}(s_{T+1}) = \frac{\sum_{t=1}^{T} b_t}{s_1} s_{T+1}. \tag{9}$$

Because b_t is nonlinear, b_{T+1} is also a nonlinear function of $\mathbf{s}$ and $\mathbf{r}$.

3.1. Taylor Approximation

Arbitrary nonlinearity in the objective function often increases computational requirements and even makes the problem intractable. This also applies to the existing LDR approach, and ILDR is proposed to tackle this limitation. ILDR obtains an optimization problem Z^*, which can be solved by the existing LDR approach and the resulting optimal policy is also near optimal for the original problem with a nonlinear objective function. To do so, $h_t(s_t, r_t)$ is approximated by its first-order Taylor expansion. At point $(\tilde{s}_t, \tilde{r}_t)$, this linear approximation, denoted by $\tilde{h}_t(s_t, r_t, \tilde{s}_t, \tilde{r}_t)$ is,

$$\tilde{h}_t(s_t, r_t, \tilde{s}_t, \tilde{r}_t)$$
$$\triangleq h_t(\tilde{s}_t, \tilde{r}_t) + (s_t - \tilde{s}_t)\frac{\partial h_t}{\partial s_t}(\tilde{s}_t, \tilde{r}_t) + (r_t - \tilde{r}_t)\frac{\partial h_t}{\partial r_t}(\tilde{s}_t, \tilde{r}_t).$$

Following $\tilde{h}_t$, $\tilde{b}_t$ can be defined as

$$\tilde{b}_t(s_t, r_t, \tilde{s}_t, \tilde{r}_t) \triangleq \min\left(\tilde{h}_t(s_t, r_t, \tilde{s}_t, \tilde{r}_t), b_t^{max}\right). \tag{10}$$

If we further fix $\dfrac{\sum_{t=1}^{T} b_t}{s_1}$ in (9) as $\tilde{\alpha}$, problem (1) becomes

$$Z = \max_{\mathbf{r}} E_{\mathbf{q}}\left[\sum_{t=1}^{T}\tilde{b}_t(s_t, r_t, \tilde{s}_t, \tilde{r}_t) + \tilde{\alpha}s_{T+1}\right], \tag{11a}$$

$$s.t. s_{t+1} = s_t + q_t - r_t, \tag{11b}$$

$$\underline{r}_t \leq r_t \leq \bar{r}_t, \quad t = 1, 2, \ldots, T, \tag{11c}$$

$$\underline{s}_t \leq s_t \leq \bar{s}_t, \quad t = 1, 2, \ldots, T+1. \tag{11d}$$

Problem (11) can be effectively approximated as a tractable SOCP problem by the existing LDR approach and this claim will be discussed in section 3.3. The parameters that identify (11) are

$$\tilde{\mathbf{r}} \triangleq [\tilde{r}_1, \tilde{r}_2, \ldots, \tilde{r}_T]', \tag{12}$$

$$\tilde{\mathbf{s}} \triangleq [\tilde{s}_1, \tilde{s}_2, \ldots, \tilde{s}_T]', \tag{13}$$

and $\tilde{\alpha}$. Each set of these parameters $\{\tilde{\mathbf{r}}, \tilde{\mathbf{s}}, \tilde{\alpha}\}$ defines a problem $Z(\tilde{\mathbf{r}}, \tilde{\mathbf{s}}, \tilde{\alpha})$, which can be solved by the existing LDR approach.

The question is how to find $\tilde{\mathbf{r}}^*, \tilde{\mathbf{s}}^*, \tilde{\alpha}^*$ such that the solution for $Z(\tilde{\mathbf{r}}^*, \tilde{\mathbf{s}}^*, \tilde{\alpha}^*)$ approximates the solution of (1). *Yoo* [2009] also uses Taylor expansion to linearize the hydro-power generation function, but he assumes that the expansion points ($\tilde{\mathbf{r}}^*, \tilde{\mathbf{s}}^*, \tilde{\alpha}^*$ in our study) are known before the optimization and this leads to an over simplified problem.

3.2. Iteration Scheme

The principles of the iteration are first explained, which are followed by the description of the iteration process.

A candidate set of parameters $\tilde{\mathbf{r}}, \tilde{\mathbf{s}}$, and $\tilde{\alpha}$ determines a candidate optimization problem $Z(\tilde{\mathbf{r}}, \tilde{\mathbf{s}}, \tilde{\alpha})$, and the solution of $Z(\tilde{\mathbf{r}}, \tilde{\mathbf{s}}, \tilde{\alpha})$ is a release policy. If this policy is applied to a sample path of inflows, the realized values of $\mathbf{r}, \mathbf{s}$, and $\alpha = \dfrac{\sum_{t=1}^{T} b_t}{s_1}$ can be calculated. For concave objective functions, the correctly chosen parameters, $\tilde{\mathbf{r}}, \tilde{\mathbf{s}}$, and $\tilde{\alpha}$, should be close to their realized values, $\mathbf{r}, \mathbf{s}$, and α. To understand this, consider the deterministic case under which there exists a static optimal policy $\mathbf{r}^*$ and the corresponding $\mathbf{s}^*$. If the chosen parameters $\tilde{\mathbf{r}}$ and $\tilde{\mathbf{s}}$ are different from $\mathbf{r}^*$ and $\mathbf{s}^*$, the gradient at $(\tilde{\mathbf{r}}, \tilde{\mathbf{s}})$ is nonzero and it points toward $(\mathbf{r}^*, \mathbf{s}^*)$. The Taylor's approximation is the same as the tangent line of the objective function at the expansion point $(\tilde{\mathbf{r}}, \tilde{\mathbf{s}})$, and the optimization problem with this Taylor's expansion will give a solution on the direction from $(\tilde{\mathbf{r}}, \tilde{\mathbf{s}})$ toward $(\mathbf{r}^*, \mathbf{s}^*)$. If we expand the nonlinear objective at this solution, a new trial starts. This iteration will eventually stop when the expansion point $(\tilde{\mathbf{r}}, \tilde{\mathbf{s}})$ is close enough to the origin point (where the gradient equals to zero) of the gradient, which is also the optimal solution $(\mathbf{r}^*, \mathbf{s}^*)$. Following the discussion on this deterministic case, we design the iteration for the stochastic optimization problem as follows.

1. Start with initial parameters $\tilde{\alpha}^0 = 0$, $[\tilde{s}_1^0, \tilde{s}_2^0, \ldots, \tilde{s}_T^0]' = \left[\frac{\bar{s}_1 + \underline{s}_1}{2}, \frac{\bar{s}_2 + \underline{s}_2}{2}, \ldots, \frac{\bar{s}_T + \underline{s}_T}{2}\right]'$, and $[\tilde{r}_1^0, \tilde{r}_2^0, \ldots, \tilde{r}_T^0]' = [\hat{q}_1, \hat{q}_2, \ldots, \hat{q}_T]'$, where $\hat{q}_t$ is the average inflow in time period t. Set $it = 0$ and go to step (1).

2. Solve the problem Z^{it} (see formulation (15)) with parameters $\tilde{\alpha}^{it}$, $[\tilde{s}_1^{it}, \tilde{s}_2^{it}, \ldots, \tilde{s}_T^{it}]'$ and $[\tilde{r}_1^{it}, \tilde{r}_2^{it}, \ldots, \tilde{r}_T^{it}]'$ to obtain the optimal release policy $\mathbf{r}^{it} = [r_1^{it}(\mathbf{q}_1), r_2^{it}(\mathbf{q}_2), \ldots, r_T^{it}(\mathbf{q}_T)]'$. Go to step (2).

3. Implement the optimal rule $\mathbf{r}^{it}$ from step (1) with the inflows $[\hat{q}_1, \hat{q}_2, \ldots, \hat{q}_T]'$ and calculate the storage and release in each of the T periods. Assign them to $[\tilde{s}_1^{it+1}, \tilde{s}_2^{it+1}, \ldots, \tilde{s}_{T+1}^{it+1}]'$ and $[\tilde{r}_1^{it+1}, \tilde{r}_2^{it+1}, \ldots, \tilde{r}_T^{it+1}]'$, respectively. Calculate the approximated generation $[\tilde{b}_1^{it}, \tilde{b}_2^{it}, \ldots, \tilde{b}_T^{it}]'$ and real generation $[b_1^{it}, b_2^{it}, \ldots, b_T^{it}]'$. $\tilde{\alpha}^{it+1} = \frac{\sum_{t=1}^{T} b_t^{it}}{T}$. Go to step (3).

4. Calculate the iteration error δ^{it} as the sum of the four relative errors in (14). $\delta^{it} \triangleq \delta_s^{it} + \delta_r^{it} + \delta_b^{it} + \delta_{\tilde{b}}^{it}$, where

$$\delta_s^{it} \triangleq \frac{\sqrt{\sum_{t=1}^{T+1}(\tilde{s}_t^{it+1} - \tilde{s}_t^{it})^2}}{\sqrt{\sum_{t=1}^{T+1}(s_t^{it})^2}}, \delta_r^{it} \triangleq \frac{\sqrt{\sum_{t=1}^{T}(\tilde{r}_t^{it+1} - \tilde{r}_t^{it})^2}}{\sqrt{\sum_{t=1}^{T}(r_t^{it})^2}},$$

$$\delta_b^{it} \triangleq \frac{\sqrt{\sum_{t=1}^{T}(b_t^{it+1} - b_t^{it})^2}}{\sqrt{\sum_{t=1}^{T}(b_t^{it})^2}}, \delta_{\tilde{b}}^{it} \triangleq \frac{\sqrt{\sum_{t=1}^{T}(\tilde{b}_t^{it+1} - \tilde{b}_t^{it})^2}}{\sqrt{\sum_{t=1}^{T}(\tilde{b}_t^{it})^2}}.$$

(14)

Record the error from linearization as $\delta_L^{it} \triangleq \frac{\sqrt{\sum_{t=1}^{T}(\tilde{b}_t^{it} - b_t^{it})^2}}{\sqrt{\sum_{t=1}^{T}(b_t^{it})^2}}$, where the subscript "L" represents lineariza-

tion. Go to step (4).

5. If $\delta^{it} > tolerance$, set $it = it+1$ and go to step (1). Otherwise, stop.

It can be seen that, there are four series of convergences:

i. $[r_1^{it}, r_2^{it}, \ldots, r_T^{it}]'$ converges to $[r_1^*, r_2^*, \ldots, r_T^*]'$,

ii. $[s_1^{it}, s_2^{it}, \ldots, s_T^{it}, s_{T+1}^{it}]'$ converges to $[s_1^*, s_2^*, \ldots, s_T^*, s_{T+1}^*]'$,

iii. $[\tilde{b}_1^{it}, \tilde{b}_2^{it}, \ldots, \tilde{b}_T^{it}]'$ converges to $[\tilde{b}_1^*, \tilde{b}_2^*, \ldots, \tilde{b}_T^*]'$,

iv. $[b_1^{it}, b_2^{it}, \ldots, b_T^{it}]'$ converges to $[b_1^*, b_2^*, \ldots, b_T^*]'$.

In step (0), the initial parameters can be any feasible values and we choose the middle points of the feasible ranges. The sample path in step (2) is chosen to be $[\hat{q}_1, \hat{q}_2, \ldots, \hat{q}_T]'$. This is because the realized optimal releases $[r_1^{it+1}, r_2^{it+1}, \ldots, r_T^{it+1}]'$ calculated in iteration step (2) is affected by the sample path used, and the iteration process converges faster by using the average inflows, $[\hat{q}_1, \hat{q}_2, \ldots, \hat{q}_T]'$, as compared with an arbitrary sample path. For step (3), although δ_L^{it} is not included in δ^{it}, it monitors the accuracy of the Taylor's approximation. We observe that δ_L^{it} generally decreases through the iteration process and when the iteration stops, δ_L^{it} is also smaller than *tolerance*.

The approximated generation $[\tilde{b}_1^{it}, \tilde{b}_2^{it}, \ldots, \tilde{b}_T^{it}]'$ is calculated by formula (10) and true generation $[b_1^{it}, b_2^{it}, \ldots, b_T^{it}]'$ is calculated by (5) and (6). In step (3), the iteration error δ^{it} is designed such that $\mathbf{s}^{it}, \mathbf{r}^{it}, \mathbf{b}^{it}$, and $\tilde{\mathbf{b}}^{it}$ all converge when the iteration stops. Furthermore, in the numerical study with *tolerance* = 0.001, we observe that δ_L^{it} is also less than the *tolerance* when the iteration stops. This means $[\tilde{b}_1^*, \tilde{b}_2^*, \ldots, \tilde{b}_T^*]'$ is close to $[b_1^*, b_2^*, \ldots, b_T^*]'$ and the Taylor's approximation is also converging to the original hydropower function. Furthermore, $\tilde{\alpha}^{it}$ automatically converges to $\tilde{\alpha}^*$ when $[b_1^{it}, b_2^{it}, \ldots, b_T^{it}]'$ converges to $[b_1^*, b_2^*, \ldots, b_T^*]'$.

3.3. Linear Decision Rule Formulation
In iteration it, Z^{it} is formulated as:

$$\max_{\mathbf{r}} E_{\mathbf{q}}\left[\sum_{t=1}^{T} u_t + \tilde{b}_{T+1}(s_{T+1})\right], \tag{15a}$$

$$s.t. \ s_{t+1} = s_t + q_t - r_t, \ t = 1, 2, \ldots, T, \tag{15b}$$

$$\underline{r}_t \leq r_t \leq \bar{r}_t, \ t = 1, 2, \ldots, T, \tag{15c}$$

$$\underline{s}_t \leq s_t \leq \bar{s}_t, \ t = 1, 2, \ldots, T+1, \tag{15d}$$

$$u_t \leq \tilde{h}_t, u_t \leq b_t^{max}, \ t = 1, 2, \ldots, T. \tag{15e}$$

where constraint (15e) follows from the fact that $\tilde{b}_t = \min(\tilde{h}_t, b_t^{max})$ is a concave piecewise linear function of s_t and r_t. Constraint (15d) is from the physical limitations of the reservoir. It integrates some other functions of the reservoir, such as flood control and irrigation. Modeling it as a hard constraint in the robust optimization formulation would mean s_t must stay in $[\underline{s}_t, \bar{s}_t]$ under any circumstances. This can make the optimization over conservative. Alternatively, they can be modeled as soft constraints—penalties in the objective function. And the penalty coefficient M is set to be sufficiently large such that the maximum possible gain in energy generation by violating those constraints is less than the penalty of the violation. In fact, constraint (15d) is rarely violated in the numerical experiments and the violation amount is less than 0.001 units. After the above reformulation, the problem becomes

$$\max_{\mathbf{r} \in \mathcal{R}} E_{\mathbf{q}}\left[\sum_{t=1}^{T}(u_t - M(s_{t+1} - \bar{s}_{t+1})^{+} - M(\underline{s}_{t+1} - s_{t+1})^{+}) + \tilde{\alpha}^{\star}(\bar{s}_{T+1} - (\bar{s}_{T+1} - s_{T+1})^{+})\right], \tag{16a}$$

$$s.t. \ s_{t+1} = s_t + q_t - r_t, \ \forall t = 1, 2, \ldots, T, \tag{16b}$$

$$u_t \leq \tilde{h}_t, \ \forall t = 1, 2, \ldots, T, \tag{16c}$$

$$u_t \leq b_t^{max}, \ \forall t = 1, 2, \ldots, T, \tag{16d}$$

$$r_t \geq \underline{r}_t, \ \forall t = 1, 2, \ldots, T, \tag{16e}$$

$$r_t \leq \bar{r}_t, \ \forall t = 1, 2, \ldots, T, \tag{16f}$$

$$\mathbf{u}, \mathbf{r}, \mathbf{s} \geq 0. \tag{16g}$$

The notation $(x)^{+} = \max(0, x)$ and the term $\tilde{\alpha}^{\star}(\bar{s}_{T+1} - (\bar{s}_{T+1} - s_{T+1})^{+})$ is from

$$\tilde{b}_{T+1}(s_{T+1}) = \tilde{\alpha}^{\star}\min(s_{T+1}, \bar{s}_{T+1}) = \tilde{\alpha}^{\star}(\bar{s}_{T+1} - (\bar{s}_{T+1} - s_{T+1})^{+}).$$

It has been discussed that r_t and s_t are functions of the hydrologic variable $\mathbf{q}_t$ in equations (3) and (4). b_t is a function of r_t and s_t and thus a function of $\mathbf{q}_t$. u_t inherits from b_t the dependency on $\mathbf{q}_t$. These "wait and see" decisions in a multiperiod stochastic optimization problem are called recourse decisions and their coefficient matrix in the equality constraint is called recourse matrix. In formulation (16), r_t, s_t, u_t are all recourse decision variables. The coefficient matrix corresponding to r_t, s_t, u_t in constraints (16b) is the recourse matrix. Since all the entries in the recourse matrix are constant numbers, the problem is a fixed recourse problem. These recourse decisions are functions, which are in an infinite dimensional space. The idea of LDR is to restrict them as linear functions of the hydrologic variable $\mathbf{q}_t$ and the recourse decisions would be in a finite dimensional space. To be specific,

$$r_t(\mathbf{q}_t) = r_t^{-1} + \sum_{k=0}^{t-1+f} r_t^k q_k, \tag{16}$$

where $r_t^{-1}, r_t^0, \ldots, r_t^{t-1+f}$ are the decision variables in the LDR formulation. The superscript $-1, 0, \ldots, k, \ldots, t-1+f$ correspond to the intercept and the coefficients of $\mathbf{q}_t$. Similarly, the LDR for the other recourse variables is defined as:

$$s_t(\mathbf{q}_t) = s_t^{-1} + \sum_{k=0}^{t-1+f} s_t^k q_k, \tag{18a}$$

$$u_t(\mathbf{q}_t) = u_t^{-1} + \sum_{k=0}^{t-1+f} u_t^k q_k. \tag{18b}$$

Plugging (16), (18a), and (18b) into formulation (16) will give the initial LDR formulations whose decision variables are the coefficients in (16), (18a), and (18b). The searching space is no longer an infinite-dimensional functional space. In addition to this dimension reduction, recent advance in RO has developed techniques, which can successfully solve the LDR reformulation of (1) with a linear benefit function $b_t(\cdot)$. To introduce these techniques, we first analyze how LDR exists in the problem. For simplicity of notations, a general LDR is defined as

$$y(\mathbf{q}) = y^{-1} + \sum_{k=0}^{m} y^k q_k, \tag{19}$$

where m is a positive integer. In our formulation, $y(\mathbf{q})$ exists in four formats:

$$\mathbb{E}[y^{-1} + \sum_{k=0}^{m} y^k q_k], \tag{20a}$$

$$\mathbb{E}[(y^{-1} + \sum_{k=0}^{m} y^k q_k)^+], \tag{20b}$$

$$y^{-1} + \sum_{k=0}^{m} y^k q_k = 0, \text{ for all possible inflows}, \tag{20c}$$

$$y^{-1} + \sum_{k=0}^{m} y^k q_k \geq 0, \text{ for all possible inflows}, \tag{20d}$$

where (20a) and (20b) are from the objective function (16a); (20c) is from constraints (16b) to (16f); (20d) is from constraint (16g). Because of q_t, these four formats are not tractable. Some assumptions and techniques are needed to derive their tractable counterparts.

It has been claimed that LDR policies are immunized against inaccurate uncertainty assumptions. This has been discussed by *Goh and Sim* [2010] and the main reason is that no specific probability density function is needed. However, our approach does require some readily available distributional information. The smallest and largest values can be observed or estimated. These two values give the range of the uncertainty value which is called the box support. The mean values and covariance matrix can also be calculated given sufficient amount of data. To sum up,

Assumption 1. It is assumed that q_t is not degenerate, i.e., not single-valued and it is bounded. The support of $\mathbf{q}$, denoted by $\mathcal{W}$, can be written as, $\mathcal{W} = \{\mathbf{q} | q_t \in [\underline{q}_t, \bar{q}_t], \underline{q}_t < \bar{q}_t\}$.

Assumption 2. It is further assumed that the expectation and covariance matrix of $\mathbf{q}$ are known as $\hat{\mathbf{q}}$ and Σ, respectively.

Assumption 2 directly calculates the expectation in format (20a), $E[y^{-1} + \sum_{k=0}^{m} y^k q_k] = y^{-1} + \sum_{k=0}^{m} y^k \hat{q}_k$. Optimization problems with terms in the form of (20b), (20c), or (20d) are not tractable when the uncertainties scenarios are infinite. They will be approximated by functions in some deliberately constructed function class and lead to tractable optimization problems under some uncertainty sets capturing the limited distributional information. The resulting optimization problems are named as the robust counterparts of the original optimization problem because the optimal solutions derived from the tractable optimization problems are the best against the worst case distributions in the uncertainty set. The techniques to derive these robust counterparts are presented in section A1 of Appendix A.

After deriving the above robust counterparts, we have the following theorem.

Theorem 1. Under Assumptions 1 and 2, there exists a Second-Order Cone Problem Z_{LDR}, formulated by the LDR techniques, which is a tight and tractable approximation for $\bar{Z}$.

The proof is sketched in section A1 of Appendix A1. Since a Second-Order Cone Problem can be solved efficiently in practice and in polynomial time in theory, our distributionally robust LDR provides a tractable method to solve the nonlinear, dynamic, and stochastic reservoir operations problem.

3.4. Segregated Linear Decision Rules

While the Linear Decision Rule formulation (A1a) in Appendix A leads to a tractable SOCP, the linear restriction on the solution space can make its performance substantially undermined or even result in infeasible formulations (see e.g., Example 1 in *Chen and Zhang* [2009]). To improve the performance and maintain tractability, a larger solution space is considered, where each candidate policy **y** is a piecewise linear function of **q**. Based on the work by *Chen et al.* [2008] and *Goh and Sim* [2010], each original uncertainty $q_t, t=0,$ $\ldots, T$ can be segregated into multiple uncertainties.

Suppose the support of q_t is $[\underline{q}_t, \bar{q}_t]$, where $\underline{q}_t$ can be $-\infty$ and $\bar{q}_t$ can be $+\infty$. Given a partition $(\tau_0^t, \tau_1^t, \ldots, \tau_{N_t}^t)$ of $[\underline{q}_t, \bar{q}_t]$ with $\underline{q}_t = \tau_0^t < \tau_1^t < \ldots < \tau_{N_t-1}^t < \tau_{N_t}^t = \bar{q}_t$, the segregated uncertainties from q_t can be written as $\zeta^t \triangleq \{\zeta_j^t(q_t)\}_{j=0}^{N_t}$:

$$\zeta_j^t(q_t) = \begin{cases} 1, & \text{if } j=0, \\ \tau_{j-1}^t, & \text{if } q_t \leq \tau_{j-1}^t, \quad j=1,\ldots,N_t, \\ \tau_j^t, & \text{if } q_t \geq \tau_j^t, \quad j=1,\ldots,N_t, \\ q_t, & \text{otherwise}, \quad j=1,\ldots,N_t, \end{cases}$$

where we write "(q_t)" in $\zeta_j^t = \zeta_j^t(q_t)$ to emphasize the dependency of ζ_j^t on q_t.

Figure 1 shows an example with $N_t = 7$ and $\tau_4^t \leq q_t \leq \tau_5^t$. Notice that the partition points $(\tau_0^t, \tau_1^t, \ldots, \tau_{N_t}^t)$ are not necessarily evenly distributed.

After segregation, there will be T uncertainty vectors $\zeta^t, t=1,\ldots,T$, which are stacked together as a vector ζ. It is not difficult to see $q_t = \sum_{j=1}^{N_t} \zeta_j^t - \sum_{k=1}^{N_t-1} \tau_k^t \triangleq F_t\zeta$ where $F_t = [0,\ldots,0, -\sum_{k=1}^{N_t-1} \tau_k^t, 1, 1, \ldots, 1, 0, \ldots, 0]$. A matrix F can be constructed such that the tth row of F is the row vector F_t, thus **q**$=F\zeta$. The LDR on the segregated uncertainties ζ can be written as $\beta_0 + \sum_{i=1}^{N} \sum_{j=1}^{N_i} \beta_{ij}\zeta_j^i$, which can be seen as a piecewise linear function of the original uncertainty **q** since $\beta_0 + \sum_{t=1}^{T} \sum_{j=1}^{N_t} \beta_{tj}\zeta_j^t = \beta_0 + \sum_{t=1}^{T} \sum_{j=1}^{N_t} \beta_{tj}\zeta_j^t(q_t)$. Thus the solution space of **y** is enlarged and the flexibility of the rules and feasibility of the model are improved. The segregated LDR formulation is basically the same as the LDR formulation except that the primitive uncertainties **q** are replaced by the segregated uncertainties $F\zeta$. And the expectation vector and covariance matrix for segregated LDR are calculated by the segregated data.

A natural way to choose the segregation partition, $(\tau_0^t, \tau_1^t, \ldots, \tau_{N_t}^t)$, is to select the points which make each interval (τ_j^t, τ_{j+1}^t) cover the same number of data points. This will automatically ensure that there are more segregation points for the part of support of q_t where the probability density is higher. The numerical experiments also show this choice of segregation partition performs well. The number of segregation points N_t for uncertainty q_t can be different for different t and N_t can be assigned with a larger value for the q_t which has larger standard deviation.

4. Numerical Study

In the numerical study, the computation environment for both case studies consists of Intel® Core™ i7–3770K Processor, 16 GB of RAM, Windows 7 Professional 64 Bit operating system, Matlab R2011a, IBM ILOG CPLEX 12.4 and ROME (Robust Optimization Made Easy) developed by *Goh and Sim* [2011].

4.1. Single Reservoir Case Study: The TGR

The TGR is a vital project for water resources development of China's longest river, the Yangtze River. This reservoir receives inflow from a 4.5×10^3 km long channel with a contributing drainage area of 10^6 km^2 (see Figure 2). The average annual runoff at the dam site is $4.51 \times 10^5 MillionCubicMeter (MCM)$. The TGR is to date
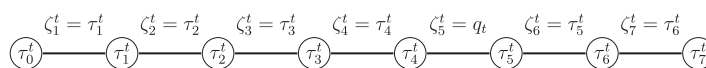
Figure 1. An example of segregation with $N_t = 7$ and $\tau_4^t \le q_t \le \tau_5^t$.

the largest multipurpose hydro-development project ever built in the world and it has an annual power-generation capacity of 84.7 billion kW h (kilowatt hours) in 2011.

Eight policies and their performance are analyzed and compared. The benchmark policy, *SP*, is calculated by SSDP which uses all the historical inflows data to derive the transition probability matrix. This gives the most advantage to SSDP when tested with inflows in history. Policy LR^i is from ILDR where $i \in \{1, 2, \ldots, 5\}$ represents the number of segregations for each uncertainty. LR^0 is from the static RO, which is not adjustable. This can be easily done by assigning zeros to all the coefficients of uncertainties. *MP* is the myopic policy which releases water as much as possible and only leaves enough water to meet the minimum storage requirement of the next period.

The performance of the policies is described by the average annual electricity generation, $\beta_n = \dfrac{\sum_{i=1}^{n} B_i}{n}$ where $B_i = \displaystyle\sum_{t=1}^{T} b_t^i$ is the sum of electricity generated in all the *T* periods of year *i*; *n* is the number of years that are studied. For historical data $n = 123$ and for generated data $n = 20,000$. Consecutive years of operation are studied. To be specific, the storage at the end of year *i* is used as the initial storage of year $i + 1$. The initial state of each year, s_1, affects the optimal policy of that year. By virtue of the structure of LDR we have developed, the first period storage s_1 can be treated as uncertain and affect the optimal policy as an independent variable.

4.1.1. Numerical Study With Historical Inflows

The data for TGR are used in this section. Even though the TGR was not constructed until the year of 2003, the inflows data from upstream rivers have been collected every 10 days for 123 years. A 10 day interval, "deka-dal," is a commonly used Chinese unit of time, called "*Xun*" in Chinese and each month is divided into three dekadals. Thus $T = 36$ for all the numerical experiments in this paper. Table 1 summarizes the performance comparison of the eight policies implemented with recorded inflows of this 123 years. The second column is the computation time in seconds; column 3 is the number of iterations needed, column three is the average annual power generation. Column 4 compares the standard deviation of the annual generation. The comparison with SSDP is measured in percentage for both column 4 and column 5. The myopic policy leads to the worst performance, which indicates careful modeling and calculation are needed for the planning.

It shows in Table 1 that the ILDR formulations can be solved within much shorter time than SSDP. To achieve 96.8% of electricity generation under the SSDP policy, LR^0 takes around 1.5% of the time by SSDP. When the
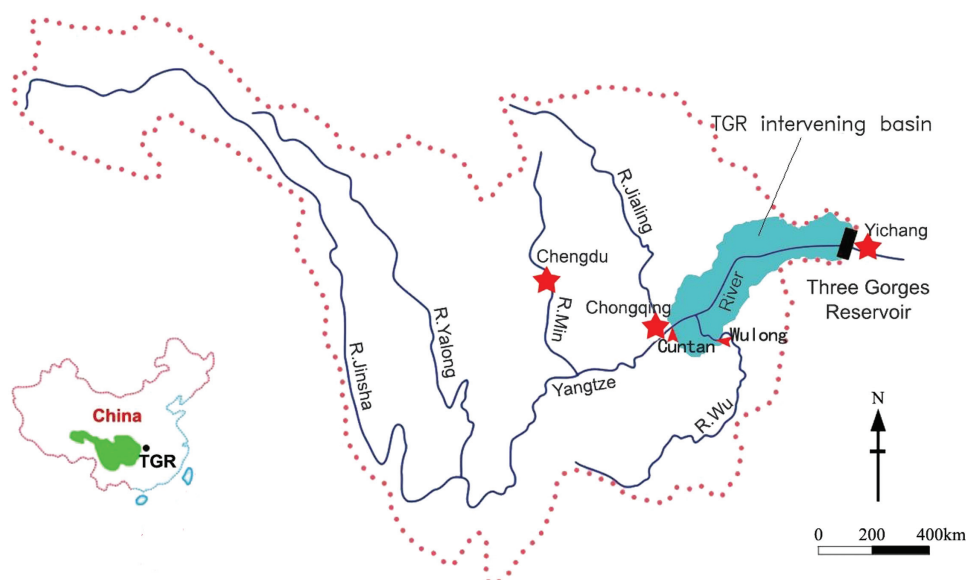
Figure 2. The location of the Three Gorges Reservoir basin in China.

Table 1. Policies Comparison With Consecutive Historical Inflows[a]

Rule	Time (s)	Iteration	β_{123}(% of SP)	STD(% of SP)
SP	1668.83		92.54(100.0%)	7.77(100.0%)
MP	0		82.24(88.9%)	7.19(92.5%)
LR^0	1.84	14	89.56 (96.8%)	7.58(97.5%)
LR^1	15.64	5	92.15(99.6%)	7.80(100.4%)
LR^2	61.01	8	92.42(99.9%)	7.47(96.1%)
LR^3	117.22	5	92.73(100.2%)	7.67(98.7%)
LR^4	201.46	5	92.74(100.2%)	7.62(98.1%)
LR^5	273.54	5	92.69(100.2%)	7.61(98.0%)

[a]Eight policies are compared, where SP refers to SSDP; MP means myopic policy; LR^i's are from ILDR and the superscript i specifies the number of segregation; LR^0 is obtained from static RO. The average annual energy generation β_{123} and the standard deviation of annual energy generation STD are both in units of billion kW h.

number of segregations increases to 2, 99.9% optimality is achieved and less than 30% of the SSDP time is needed. When the segregation increases to 3, the performance of ILDR catches up with that of SSDP.

Even with historical inflows that provide the most advantage to SSDP, the ILDR can perform as well as SSDP. This is because, due to the problem of curse of dimensionality, SSDP can only include the storage of one period in the state variable and estimates transition probability matrix by assuming a Markovian process that corresponds to AR(1) model. Statistical analysis [*Shumway and Stoffer*, 2010] shows that the inflows to TGR is best described by an (autoregressive integrated moving average) $ARIMA(4, 1, 4) \times (1, 1, 1)_{36}$ model, where (4, 1, 4) are the nonseasonal parameters: the order of the autoregressive part is 4, the order of integrated part is 1, and the order of moving average part is 4; (1, 1, 1) are the corresponding seasonal parameters; and 36 specifies the length of a cycle.

Figure 3 compares the histogram of annual generation based on the policies. The top dotted line connects the maximum annual generation in 123 years under each policy. The bottom dotted line connects the minimum annual generation. The dashed line in the middle connects the average generation. Six representative policies are included in this figure. The myopic policy gives the worst performance. The static robust optimization LR^0 is not as good as the ones on its right-hand side because it is too conservative. The third histogram is for SSDP which spreads the broadest range and has more than one instances in each "bar." The last three histograms are for the adjustable RO. As can be seen, their histograms' ranges are similar to that of SSDP. The lowest bar looks like a line segment because there is only one instance falling inside of that bar. So the worst case scenarios with adjustable ILDR are fewer than those under SSDP.

Figure 4 shows the performance of the LDR polices gradually approaches the performance of SSDP as the number of segregations increases. The dotted horizontal line at the top represents the optimal value from the problem OP, which is a deterministic optimization problem with a planning horizon including all the 123 years of history. In OP, all the values of inflows are given in the optimization. Therefore, the optimal value of OP, 96.35 billion kW h, is the maximum possible performance that any policy could achieve. The percentage increase in optimal value from the advantage of knowing future inflows is named as "value of perfect information," V_I, which can be calculated as $V_I = 1 - \frac{92.54}{96.35} = 3.95\%$ for this case study.

The setting of the problem as discussed above gives the most advantage to SSDP because the simulation is run by the same data, from which the probability transition matrix of SSDP is derived. The water inflows data set is not divided into training and validating periods because there are only 123 samples; the number is relatively small compared with the number of parameters in the decision rules of the 36 periods. In the next section, the eight policies are compared in generated data that still has the same mean and covariance as the historical inflows.

4.1.2. Distributional Robustness
In this section, three different distributions are tested:

1. Bootstrapping: Sampling 20,000 times from the 123 years with replacement. This keeps both the mean and covariance of the flows $[q_1, q_2, \ldots, q_T]$ the same as the historical data, but creates new sequences of flows.

2. Truncated normal: These artificial inflows follow a truncated normal distribution with the same mean vector and covariance matrix as the recorded inflows. The truncation is to ensure all the generated inflows are positive.

3. Exponentially distributed inflows: These inflows are sampled from an exponential distribution which has the same mean and covariance matrix as the historical inflows.
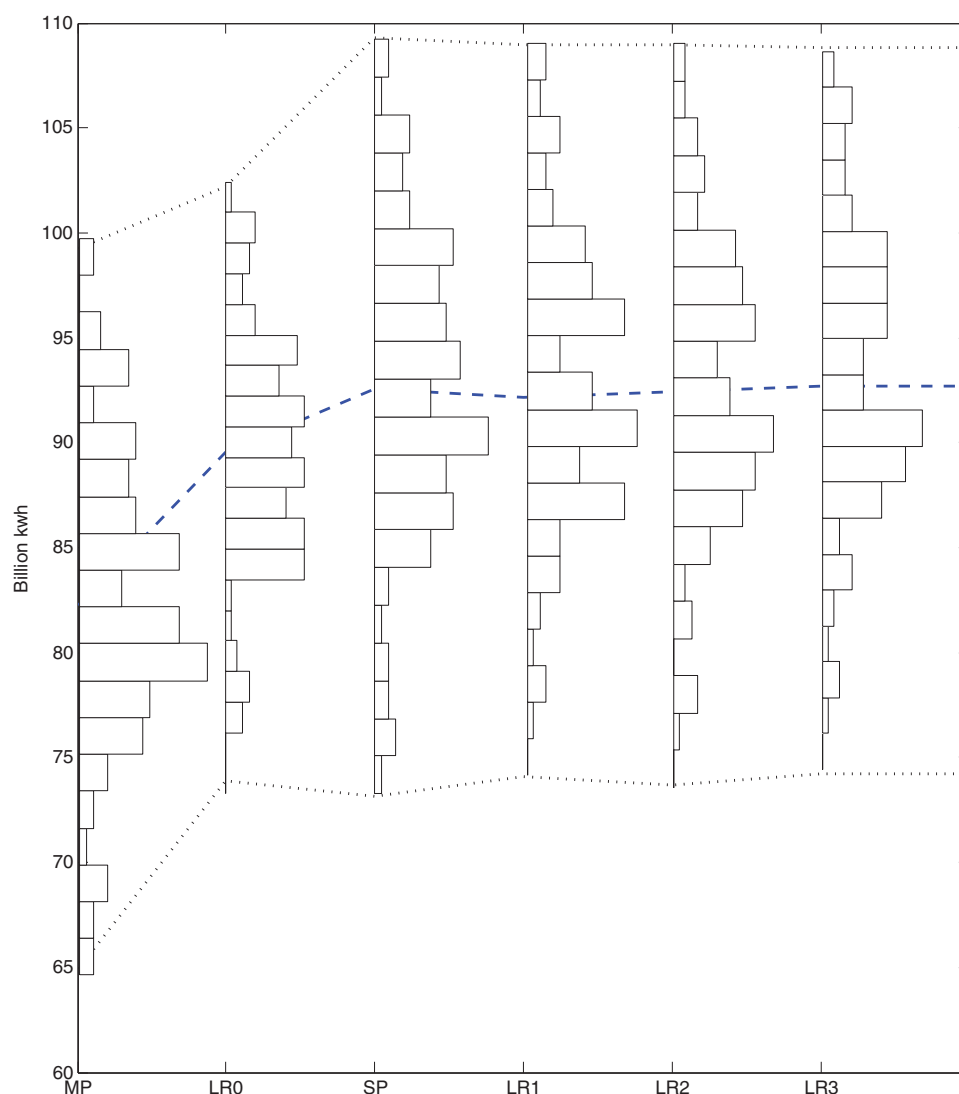
Figure 3. Histogram comparison of the policies with consecutive historical inflows. The vertical axis is for the annual electricity generation in billion kW h.

From Table 2, it can be seen that, under the generated inflows, the adjustable ILDRs (LR^i, $i \geq 1$) almost always obtain better performance than SSDP. In the Bootstrapping case, the results are very similar to the ones in the study using historical inflows. This is because bootstrapping simply reorders and repeats the years in history. When the inflows follow truncated normal distribution, LR^3, LR^4, and LR^5 generate 1.6% more electricity. This will count for almost 1.6 billion kW h of electricity given the scale of TGR. With the inflows following exponential distribution, the expected annual electricity generation from SSDP and ILDR policies are similar. The advantage of ILDR can be clearly seen from the standard deviation column. This advantage is also shown in Figure 5 where it shows that spills are reduced in intensity and frequency by LR^4. It is called potential spills because these spills will happen if the policy from optimization is strictly followed; but they are actually avoided by adjusting the release from the optimal policy. The adjustment is described in section A3 of Appendix A. The potential spills occur because the testing inflows are not identical to the historical data which generate the policies.

Another point worth mentioning is the relationship between the performance and the number of segregated pieces. While making the policy adjustable to uncertainties significantly improves the performance, increasing the number of uncertainty pieces does not always make the performance better. For instance
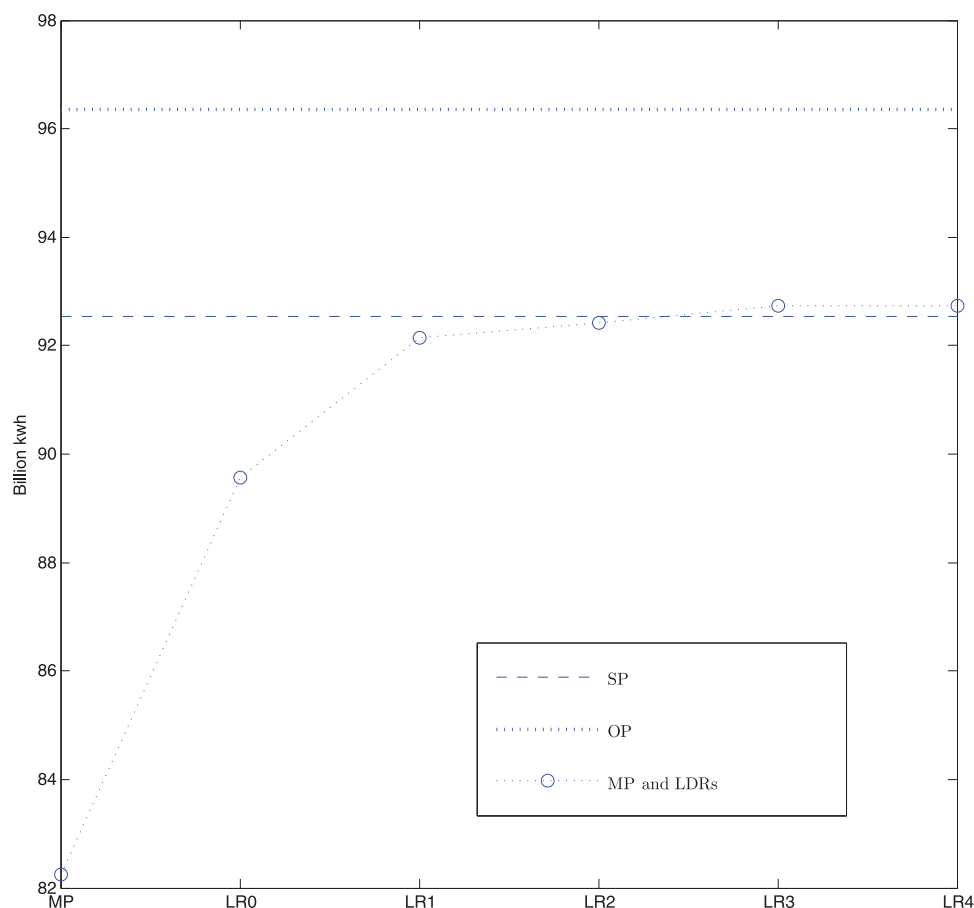
Figure 4. The performance comparison of the policies on TGR with historical inflows. The vertical axis is for the average annual electricity generation in billion kW h.

LR^4 is better than LR^5 in some cases. One reason for this phenomenon is related to the accuracy of the mean and covariance of the segregated uncertainties. One observed instance of q_t leads to N_t "observed" segregated uncertainties: $\zeta_j^t(q_t), j=1,\ldots,N_t$. N_t-1 of these segregated uncertainties lies on the segregation

Table 2. Policy Comparison With Consecutive Generated Inflows

Rule	Distribution	Mean (Billion kW h) (% of SP)	STD (Billion kW h) (% of SP)
SP	Bootstrapping	92.64(100.0%)	7.69(100.0%)
LR^0	Bootstrapping	86.03(97.24%)	7.38(95.91%)
LR^1	Bootstrapping	92.23(99.56%)	7.71(100.2%)
LR^2	Bootstrapping	92.49(99.84%)	7.62(99.09%)
LR^3	Bootstrapping	92.81(100.2%)	7.57(98.50%)
LR^4	Bootstrapping	92.82(100.2%)	7.53(97.89%)
LR^5	Bootstrapping	92.77(100.1%)	7.52(97.77%)
SP	Normal	90.98(100.0%)	7.80(100.0%)
LR^0	Normal	89.60(98.49%)	7.54(96.65%)
LR^1	Normal	92.11(101.2%)	7.19(92.18%)
LR^2	Normal	92.11(101.3%)	7.69(98.65%)
LR^3	Normal	92.48(101.6%)	7.94(101.81%)
LR^4	Normal	92.46(101.6%)	7.94(101.86%)
LR^5	Normal	92.39(101.6%)	7.90(101.24%)
SP	Exponential	119.72(100.0%)	3.75(100.0%)
LR^0	Exponential	116.56(97.4%)	3.51(97.4%)
LR^1	Exponential	120.78(100.9%)	3.43(91.5%)
LR^2	Exponential	119.09(99.5%)	3.34(89.1%)
LR^3	Exponential	119.72(100.0%)	3.10(82.7%)
LR^4	Exponential	119.89(100.1%)	3.13(83.3%)
LR^5	Exponential	119.76(100.0%)	3.15(83.9%)
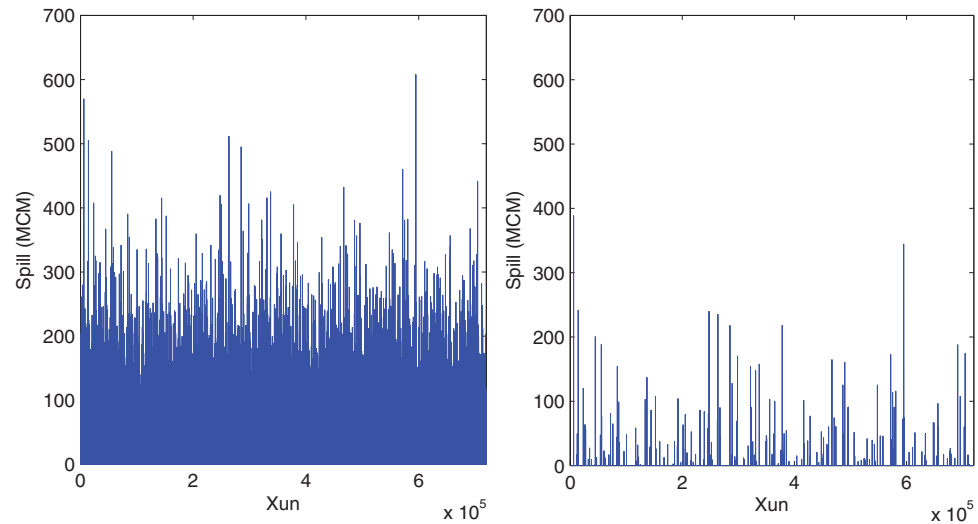
Figure 5. Potential spills (infeasibility) from SSDP and LR^4. 1 Year = 36 *Xun*.

points p_j^t (see Figure 1). In this study, when $N_t = 5$, on average there are only around 20 (out of 123) "observations" of $\zeta_j^1(q_1)$ for each j which may not be enough to derive reliable statistics. Thus the information in the expanded space is essentially no more than that in the original uncertainty space. The mean vector and covariance matrix with a larger size are not accurate when the number of segregations is too high. Therefore, it suggests that, in practice, a small number of segregation pieces should be used first and the number of segregations can be increased until the performance stops improving.

4.2. Multireservoir Case Study: The CVP

To illustrate how our method can be extended to multireservoir system, the model for Shasta-Trinity subsystem of Central Valley Project (CVP) is borrowed and modified from *Tejada-Guibert et al.* [1995]. The major difference is that *Tejada-Guibert et al.* [1995] consider the value of electricity as a function of demand while in our study, the electricity price is static. This case study is a "proof-of-concept" and it does not intend to be applied in reality.

The CVP is a federal water management project in California which diverts water from northern California and provides water to irrigation and municipal demand sites in the Central Valley. Hydroenergy generation is also an important function of CVP. As shown in Figure 6, the Shasta-Trinity consists of three reservoirs, Clair Engle, Shasta, and Whiskeytown, numbered by 1, 2, and 3; and five power plants, Trinity, Shasta, Francis Carr, Spring Creek, and Keswick, numbered with 1–5, respectively. Similar to the single reservoir model, the storage of reservoir is denoted by s^i and inflow is denoted by q_t^i, $i = 1, 2$ and $t = 1, 2, \ldots, 12$. The monthly data for these inflows from October 1912 to October 2012 are calculated from the records of stations *MSS*, *PSH*, and *TNL* of this multireservoir system. Notice that even though the inflows data include recent years, all other parameters are adopted from *Tejada-Guibert et al.* [1995] and may not reflect the current status of the CVP. Because each power plant i has a capacity $K_{i,t}$ in period t, the water travels through the turbines at this power plant, $u_{i,t}$ is restricted:

$$
u_{i,t} =
\begin{cases}
\min\left(r_{1,t}, \dfrac{K_{i,t} h_{tot,t}}{E_{i,t}^f}\right), & \text{if } i = 1, 3, 4, \\[2ex]
\min\left(r_{2,t}, \dfrac{K_{2,t} h_{tot,t}}{E_{2,t}^f}\right), & \text{if } i = 2, \\[2ex]
\min\left(r_{2,t} + u_{4,t}, \dfrac{K_{5,t} h_{tot,t} - \theta_t}{\phi_t}\right), & \text{if } i = 5,
\end{cases}
$$

where $E_{i,t}^f$ is the energy factor associated with plant i in period t; $h_{tot,t}$ is the total number of operation hours in period t; ϕ_t and θ_t are the energy coefficients of Keswick power plant in period t. $E_{i,t}^f$, $h_{tot,t}$, ϕ_t, and θ_t are all constant parameters.
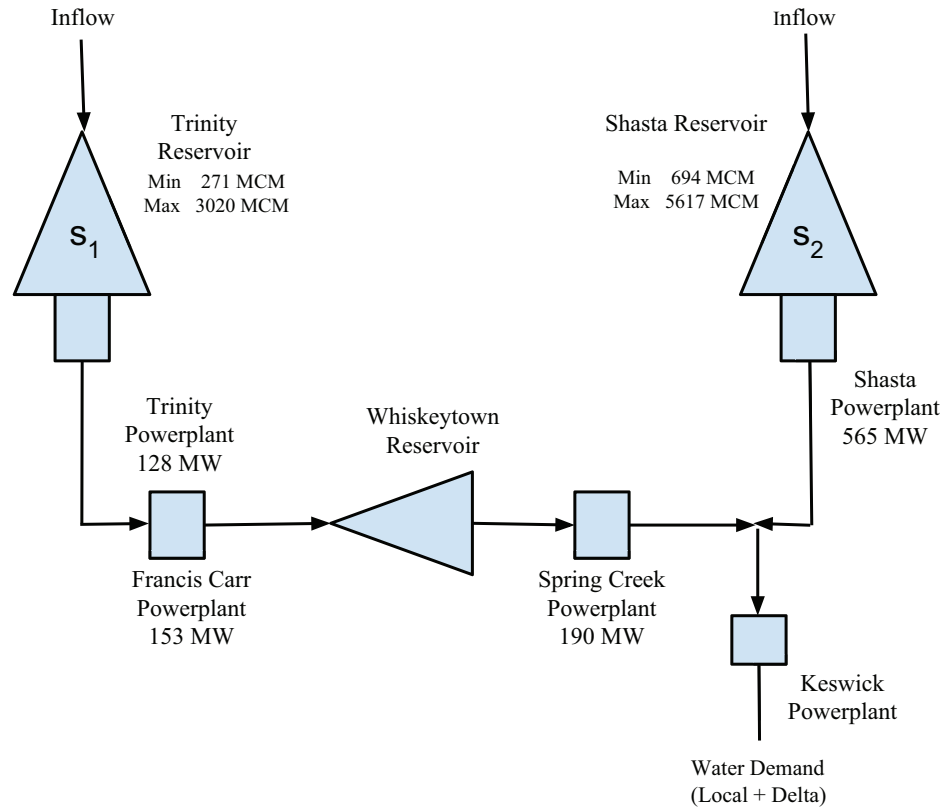
Figure 6. The schematic diagram of the Shasta-Trinity subsystem.

The Whiskeytown reservoir has sufficient storage capability and it only releases water through the turbines of plant 4, the maximum possible amount of water that can enter plant 5 is $u_{4,t}+r_{2,t}$ which is also the water to meet the downstream demand w_t. Because the first purpose of this multireservoir system is water supply, we characterize the water shortage by $SW_t \triangleq \max(0, \gamma_d w_t - u_{4,t} - r_{2,t})$ and the importance of meeting the demand can be controlled by γ_d. Following *Tejada-Guibert et al.* [1995], the power generation at plant i in period t is $u_{i,t}E_{i,t}^f$ and the system's benefit in period t is defined as

$$b_t = \sum_{i=1}^{5} u_{i,t}E_{i,t}^f - \rho SW_t,$$

where ρ controls the weight of supplying water in the objective.

To summarize, the stochastic optimization problem for this multireservoir system is

$$\tilde{Z}_{CVP}^* = \max_{\mathbf{r} \in \mathcal{R}} E_{\mathbf{q}_1,} \left[\sum_{t=1}^{12} \sum_{i=1}^{5} u_{i,t}E_{i,t}^f - \rho \max(0, \gamma_d w_t - u_{4,t} - r_{2,t}) \right] \tag{21a}$$

$$s.t. \ s_{1,t+1} = s_{1,t} + q_{1,t} - r_{1,t}, \ \forall t = 1, 2, \ldots, 12, \tag{21b}$$

$$s_{2,t+1} = s_{2,t} + q_{2,t} - r_{2,t}, \ \forall t = 1, 2, \ldots, 12, \tag{21c}$$

$$u_{i,t} \leq \frac{K_{i,t}h_{tot,t}}{E_{i,t}^f}, u_{i,t} \leq r_{1,t}, i = 1, 3, 4, \ \forall t = 1, 2, \ldots, 12, \tag{21d}$$

$$u_{2,t} \leq \frac{K_{2,t}h_{tot,t}}{E_{2,t}^f}, u_{2,t} \leq r_{2,t}, \ \forall t = 1, 2, \ldots, 12, \tag{21e}$$

Table 3. Policies Comparison With Trinity-Shasta Inflows From October 1912 to October 2012, Recorded and Artificially Generated[a]

Rule	Inflows	Time (s)	β_{100}(% of OP)	Shortage Rate (%)	STD(% of OP)
OP	History	151.3	617.96(100.0%)	0.0	92.67(100.0%)
LR^1	History	9.51	564.7(91.4%)	0.0	105.7(114.1%)
LR^2	History	36.03	584.95(94.7%)	0.0	117.13(126.4%)
LR^3	History	76.1	585.17(94.7%)	0.8	124.84(134.7%)
LR^4	History	131.73	584.82(94.6%)	0.0	124.49(134.3%)
LR^5	History	200.09	585.97(94.8%)	0.0	123.69(133.5%)
OP	Normal	152.7	637.04(100.0%)	0.0	48.83(100.0%)
LR^1	Normal	0	594.45(93.3%)	0.0	69.76(142.8%)
LR^2	Normal	0	604.97(95.0%)	0.0	74.5(152.5%)
LR^3	Normal	0	606.77(95.2%)	0.0	78.07(159.8%)
LR^4	Normal	0	613.24(96.3%)	0.0	80.41(164.6%)
LR^5	Normal	0	614.15(96.4%)	0.0	79.61(163.0%)
OP	Exponential	159.6	622.31(100.0%	0.0	79.61(100.0%)
LR^1	Exponential	0	581.42(93.4%)	0.0	70.69(88.8%)
LR^2	Exponential	0	590.49(94.9%)	0.0	67.67(85.0%)
LR^3	Exponential	0	593.65(95.4%)	0.0	71.67(90.0%)
LR^4	Exponential	0	596.27(95.8%)	0.0	73.75(92.6%)
LR^5	Exponential	0	595.82(95.7%)	0.0	73.53(92.4%)

[a]Six policies are compared, where OP refers to the policy derived when the future can be fully forecasted; LR^i's are from ILDR and the superscript i specifies the number of segregation. The average annual energy generation β_{100} and the standard deviation of annual energy generation STD are both in units of billion kW h.

$$u_{5,t} \leq r_{2,t} + u_{4,t}, u_{5,t} \leq \frac{K_{5,t} h_{tot,t} - \theta_t}{\phi_t}, \forall t = 1, 2, \ldots, 12, \tag{21f}$$

$$\underline{s}_1 \leq s_{1,t} \leq \bar{s}_{1,t}, \underline{s}_2 \leq s_{2,t} \leq \bar{s}_{2,t}, \forall t = 1, 2, \ldots, 13, \tag{21g}$$

$$\mathbf{r}, \mathbf{s}, \mathbf{u} \geq 0. \tag{21h}$$

Notice that the hydropower generation function in this case study is piecewise linear instead of polynomial as in the TGR case study. Because this case study is adopting the model from *Tejada-Guibert et al.* [1995]; however, a similar iteration can be done if the power generation function is polynomial.

Observing that, all the terms involving uncertainties, $r_{i,t}$, $s_{i,t}$, and $u_{i,t}$ are in the four formats (20a)–(20d) that have equivalent deterministic robust counterpart, this problem is ready to be converted into an SOCP by applying ILDR. Because SSDP suffers from the "curse of dimensionality" when applied to a multireservoir system, the benchmark is derived from OP, which is a deterministic optimization problem with all the inflows from October 1912 to October 2012 given. Assume $\gamma_d = 1$, which means the regular water demand is exactly matched. The weight for water demand is $\rho = 0.15$ and the weight for power generation (million kW h) is 1. Table 3 compares the performance of six policies implemented on the historical inflows from October 1912 to October 2012. The structure of Table 3 is similar to that of Tables 1 and 2 except for the column "shortage rate" which characterizes the percentage of periods when the water demand is not satisfied. LR^0 is ignored because it is not a feasible problem if the LDR is not adjustable. In Table 3, it can be seen that ILDR models the water demand term, $max(0, \gamma_d w_t - u_{4,t} - r_{2,t})$, very well and only LR^3 leads to 0.8% of shortage. The performance of LR^i improves as the number of segregations increases. It can be seen from the numerical results that the gap between ILDR and OP for a multireservoir system is similar to the gap between ILDR and OP for a single-reservoir system. Although OP is unrealistic because not all the future inflows can be forecasted, it can be used with V_I to estimate the optimal value of the true optimal policy for this stochastic optimization problem. If V_I is still 3.95% as in the single-reservoir system, the loss of optimality for ILDR method would be around 1% in the multireservoir system.

5. Conclusions

In this paper, reservoir operation optimization problems under uncertainty and with nonlinear objective functions are addressed. These problems are difficult because they are usually high-dimensional, dynamic, nonlinear, and stochastic. The distributionally robust Linear Decision Rule (LDR) is introduced and extended to Iterative Linear Decision Rule (ILDR), which is tested with both the single reservoir and multireservoir systems, and the performance of the proposed method is satisfactory compared to the SSDP and

"OP" benchmarks. The complexity and accuracy of ILDR can be adjusted by the number of segregations. The techniques and formulations of ILDR developed in this paper can be used to solve other similar problems.

Both the method derivation in section 3 and the numerical studies in section 4 assume the objective functions are concave in the maximization problems. For nonconcave objectives, the iteration process proposed in section 3 may not converge at a single set of parameters $\{\tilde{\mathbf{r}}^*, \tilde{\mathbf{s}}^*, \tilde{\alpha}^*\}$. In an artificial case study with a nonconcave objective function, we observe that the iteration process enters a cycle between two sets of parameters, $\{\tilde{\mathbf{r}}_1^*, \tilde{\mathbf{s}}_1^*, \tilde{\alpha}_1^*\}$ and $\{\tilde{\mathbf{r}}_2^*, \tilde{\mathbf{s}}_2^*, \tilde{\alpha}_2^*\}$, which may lead to two possible local optimal solutions. This is predicted behavior since local solvers can only find local optimal solutions when maximizing nonconcave problems. Nevertheless, one can search for the global maximum by exploring the set of local maxima. This set could be obtained by employing multistart optimization procedure [*Ugray et al.*, 2007] that starts the local solver from a variety of starting points (generally the starting points are random) which converge to different solutions.

Moreover, this procedure potentially broadens the capability of the proposed method. *Bertsimas and Sim* [2004] extend the linear decision rules to polynomial rules and the formulation ends with a sum-of-square (essentially a semidefinite programming) problem. Although the objective in *Bertsimas and Sim* [2004] is piecewise linear, the more general polynomial decision rules approach can be modified to solve reservoir operation problems with nonconcave objective functions. However, this polynomial decision rule approach may involve polynomials with very high degrees which make computation challenging. On the contrary, the proposed ILDR can be developed with moderate efforts through ROME [*Goh and Sim*, 2011] as shown in this study. The application of the mathematical optimization problem to both single and multireservoir systems is tractable. The tractability of the problem is obtained without compromising the performance of the optimal policy as illustrated in the results, i.e., the proposed method performs as good as SSDP. Moreover, the results demonstrate that the policy obtained from ILDR is distributionally robust in the sense that it performs well even if the PDF is not fully known.

Appendix A

A1. Linear Decision Rule Techniques

Proposition 1. If two linear decision rules are equal, their coefficients are also equal for each q_k, respectively. That is, $y^{-1} + \sum_{k=0}^{m} y^k q_k = 0$ is equivalent to $y^i = 0$, $i = -1, 0, 1, \ldots, m$.

Proof . Assume $\mathbf{q} = [q_0, \ldots, q_m]$ is an arbitrary observation of the uncertainties. By Assumption 1, for any $k \in \{0, 2, \ldots, m\}$, there exists another uncertainty vector $\mathbf{q}'$ which is only different from $\mathbf{q}$ by the component q_k. Thus we have $y(\mathbf{q}) = y(\mathbf{q}') = 0$ which leads to $y^k(q_k - q_k') = 0$ thus $y^k = 0$. ∎

Proposition 2. It has been shown in *Ben-Tal et al.* [2004] that (20d) is equivalent to the robust counterpart

$$y^{-1} + \sum_{k=0}^{T} \left(y^k \frac{\underline{q}_k + \bar{q}_k}{2} + \frac{\bar{q}_k - \underline{q}_k}{2} \theta^k \right) \leq 0, \quad -\theta^k \leq y^k \leq \theta^k.$$

In terms of (20b), a simpler upper bound for $\mathbb{E}[(y^{-1} + \sum_{k=0}^{m} y^k q_k)^+]$ can be found such that the problem becomes tractable after the upper bound is used to replace (20b). Theorem 2 in *Goh and Sim* [2010] which is generalized from Theorem 1 in *Chen et al.* [2008] can serve this purpose.

Proposition 3. Let $\mathbb{F}$ be the family of all distributions $\mathbb{P}$ such that the uncertainty vector $\mathbf{q}$ has mean $\hat{\mathbf{q}}$ and covariance matrix Σ, i.e.,

$$\mathbb{F} = \{\mathbb{P} : \mathbb{E}_{\mathbb{P}}(\mathbf{q}) = \hat{\mathbf{q}}, \mathbb{E}_{\mathbb{P}}((\mathbf{q} - \hat{\mathbf{q}})(\mathbf{q} - \hat{\mathbf{q}})') = \Sigma\}.$$

Then $\pi(y^{-1}, \mathbf{y})$ is a tight upper bound for $\mathbb{E}_{\mathbb{P}}[(y^{-1} + \mathbf{y}'\mathbf{q})^+]$ over all distributions $\mathbb{P} \in \mathbb{F}$, where

$$\pi(y^{-1}, \mathbf{y}) \triangleq \frac{1}{2}(y^{-1} + \mathbf{y}'\hat{\mathbf{q}}) + \frac{1}{2}\sqrt{(y^{-1} + \mathbf{y}'\hat{\mathbf{q}})^2 + \mathbf{y}'\Sigma\mathbf{y}}$$

and $\mathbf{y} = [y^0, y^1, \ldots, y^m]'$.

A2. Proof of Theorem 1

Apply Propositions 1, 2, and 3 to formulation (16), the expressions and constraints with uncertainties can be converted into their deterministic counterparts. Thus formulation (16) becomes

$$\hat{Z}_{SOCP} = \max \sum_{t=1}^{T} (y_{6T+t+1}^{-1} + \sum_{k=0}^{t-1+f} y_{6T+t+1}^k \hat{q}_k) - \sum_{t=1}^{T} M(\pi_t^u + M\pi_t^\ell) - \alpha\pi + \tilde{\alpha}^\star \bar{s}_{T+1}, \tag{21}$$

$$s.t. \ W^t\mathbf{y}^t = \mathbf{h}^t, \forall t \in \{0, \ldots, T\}, \tag{22}$$

$$y_t^{-1} + \sum_{k=0}^{T}(y_t^k \frac{\underline{q}_k + \bar{q}_k}{2} + \frac{\bar{q}_k - \underline{q}_k}{2}\theta_t^k) \le 0, \ -\theta_t^k \le y_t^k \le \theta_t^k,$$

$$k \in \{1, \ldots, T\}, t \in \{1, 2, \ldots, 7T+1\}, \tag{23}$$

$$\frac{1}{2}\sqrt{(y_{4T+t+1}^{-1} - \bar{s}_{t+1} + \mathbf{y}_{4T+t+1}'\hat{\mathbf{q}})^2 + \mathbf{y}_{4T+t+1}'\Sigma\mathbf{y}_{4T+t+1}} \le$$

$$\pi_t^\ell - \frac{1}{2}(-y_{4T+t+1}^{-1} - \mathbf{y}_{4T+t+1}'\hat{\mathbf{q}}), t \in \left\{1, 2, \ldots, T\right\}, \tag{24}$$

$$\frac{1}{2}\sqrt{(\underline{s}_{t+1} - y_{4T+t+1}^{-1} - \mathbf{y}_{4T+t+1}'\hat{\mathbf{q}})^2 + \mathbf{y}_{4T+t+1}'\Sigma\mathbf{y}_{4T+t+1}} \le$$

$$\pi_t^u - \frac{1}{2}(-\underline{s}_{t+1} + y_{4T+t+1}^{-1} + \mathbf{y}_{4T+t+1}'\hat{\mathbf{q}}), t \in \left\{1, 2, \ldots, T\right\}, \tag{25}$$

$$\frac{1}{2}\sqrt{(\bar{s}_{T+1} - y_{5T+1}^{-1} - \mathbf{y}_{5T+1}'\hat{\mathbf{q}})^2 + \mathbf{y}_{5T+1}'\Sigma\mathbf{y}_{5T+1}} \le$$

$$\pi - \frac{1}{2}(-\bar{s}_{T+1} + y_{5T+1}^{-1} + \mathbf{y}_{5T+1}'\hat{\mathbf{q}}). \tag{26}$$

where $\mathbf{y}_t = [y_t^1, y_t^2, \ldots, y_t^T]'$ and $\mathbf{y}^t = [y_1^t, y_2^t, \ldots, y_{7T+1}^t]'$. W^t and $\mathbf{h}^t$ is constructed by comparing the coefficients on the two sides of equality constraints in formulation (16).

A3. Adjustment After Optimization

The idea is to adjust the policy from the optimization whenever it violates the constraints in the simulation. There are two types of possible violations:

a. violations of the constraints for r_t;

b. violations of the constraints for s_t;

First, r_t has to be between its lower and upper bounds because they are physical hard constraints, that is $r_t^a = \max(\min(\bar{r}_t, r_t), \underline{r}_t)$, here the "tilde" sign on the top of a decision variable means that this decision has been adjusted. After these two constraints are satisfied, r_t is adjusted based on the optimal solution and the type of violations from constraints on s. To be more specific:

(0) if $s_{t+1} > \bar{s}_{t+1}$, then

$$r_t^a = \min(\bar{r}_t, q_t - \bar{s}_{t+1} + s_t),$$
$$s_{t+1}^a(r_t^a) = s_t + q_t - r_t^a,$$

(1) if $s_{t+1} < \underline{s}_{t+1}$, then

$$r_t^a = \max(\underline{r}_t, q_t - \underline{s}_{t+1} + s_t),$$
$$s_{t+1}^a(r_t^a) = s_t + q_t - r_t^a,$$

(2) if $r_t > \bar{r}_t$, then

$$r_t^a = \bar{r}_t,$$

$$s_{t+1}^a(r_t^a) = s_t + q_t - r_t^a,$$

(3) if $r_t < \underline{r}_t$, then

$$r_t^a = \underline{r}_t,$$

$$s_{t+1}^a(r_t^a) = s_t + q_t - r_t^a.$$

By virtue of the above adjustment, the constraints for both r_t and s_t can always be satisfied in the numerical experiments.

A4. Sampling Stochastic Dynamic Programming

The following sampling stochastic dynamic programming (SSDP) approach is derived to generate a benchmark policy for comparison purpose. The discretizations in the SSDP are made bushier until the performance stops improving thus the policy from SSDP is considered optimal.

$$V_t = \max_{s_{t+1}} \mathbb{E}[B_t(s_{t+1}, s_t, q_t) + V_{t+1}], t = 1, 2, \ldots, T-1, \tag{A2}$$

and $V_T = \max_{s_{T+1}} \mathbb{E}[B_T]$. Unlike in the LDR formulations, where the optimal policy is in the form of optimal water release r_t, in SSDP model s_{t+1} is used as the decision variable and it is a function of the previous storage level s_t and water inflow q_t:

$$s_{t+1} = s_{t+1}(s_t, q_t), \tag{A3}$$

The inflow q_t in each time period t is uncertain and $q_t \in [\underline{l}_t, \bar{l}_t]$ where $-\infty < \underline{l}_t \leq \bar{l}_t < +\infty$. q_t is discretized into N_q intervals by dividing points $q_t^0, q_t^1, \ldots, q_t^{N_q}, \underline{q}_t = q_t^0 \leq q_t^1 \leq \ldots \leq q_t^{N_q} = \overline{q}_t$. Denote P_t^i as the probability of $q_t \in [q_t^i, q_t^{i+1})$ for $i = 0, 1, \ldots, N_q - 1$ and $P_t^{N_q}$ is the probability of $q_t = q_t^{N_q}$. Denote $P_t^{i,j}$ as the probability of $q_{t+1} \in [q_{t+1}^{i-1}, q_{t+1}^j)$ given $q_t \in [q_t^{i-1}, q_t^i]$. Both P_t^i and $P_t^{i,j}$ can be determined by the historical streamflow data; s_t is the average storage level in time period t and s_t must be in an interval of $[\underline{s}_t, \bar{s}_t]$ which is discretized into N_S smaller intervals.

By backward induction, the optimal rule s_{t+1} is calculated as a discrete function of storage level and water inflow in time period t. For example, the optimal rule $s_{T+1}^*(s_T, q_T) = s_{T+1}^*(s_T^i, q_T^j)$ is easy to calculate for all the combinations of $i \in \{0, 1, \ldots, N_s\}$ and $j \in \{0, 1, \ldots, N_q\}$. Thus, $s_{T+1}^*(s_T^i, q_T^j)$ is obtained to maximize $B_T(s_{T+1}^*(s_T^i, q_T^j), s_T^i, l_T^j)$ for all the possible (i, j) which gives a discrete function from $\{s_T^0, \ldots, s_T^{N_S}\} \times \{q_T^0, \ldots, q_T^{N_q}\}$ to $\{s_{T+1}^0, \ldots, s_{T+1}^{N_S}\}$ and $V_T(s_T^i) = \sum_{j=0}^{N_q} P_T^j B_T(s_{T+1}^*(s_T^i, q_T^j), s_T^i, l_T^j)$. Here the "$(s_T^i)$" in $V_T(s_T^i)$ is to emphasize that the value of V_T is affected by the value of s_T^i. Next, $s_T^*(s_{T-1}^i, q_{T-1}^j) \in \{s_{T-1}^0, \ldots, s_{T-1}^{N_S}\}$ for all possible (i, j) are determined by solving the following problem:

$$V_{T-1}(s_{T-1}^i) = \max_{s_T} \sum_{j=0}^{N_q} P_{T-1}^j [B_{T-1}(s_T(s_{T-1}^i, q_{T-1}^j), s_{T-1}^i, l_{T-1}^j) + \sum_{k=0}^{N_q} P_{T-1}^{j,k} B_T(s_{T+1}^*(s_T, q_T^k), s_T, l_T^k)] \tag{A4}$$

Continue the above process until time period 1 is finished.

References

Ben-Tal, A., A. Goryashko, and A. N. E. Guslitzer (2004), Adjustable robust solutions of uncertain linear programs, *Math. Program.*, *99*(2), 351–376.

Ben-Tal, A., L. El Ghaoui, and A. Nemirovski (2009), *Robust Optimization*, Princeton Univ. Press, Princeton University Press, Princeton, N. J.

Bertsimas, D., and M. Sim (2004), The price of robustness, *Oper. Res.*, *52*(1), 35–53.

Bhaskar, N. R., and E. E. Whitlatch (1987), Comparison of reservoir linear operation rules using linear and dynamic programming, *Water Resour. Res.*, *23*(6), 1027–1036.

Cervellera, C., V. C. Chen, and A. Wen (2006), Optimization of a large-scale water reservoir network by stochastic dynamic programming with efficient state space discretization, *Eur. J. Oper. Res.*, *171*(3), 1139–1151.

Chen, X., and Y. Zhang (2009), Uncertain linear programs: Extended affinely adjustable robust counterparts, *Oper. Res.*, *57*(6), 1469–1482.

Chen, X., M. Sim, and P. Sun (2007), A robust optimization perspective on stochastic programming, *Oper. Res.*, *55*(6), 1058–1071.

Chen, X., M. Sim, P. Sun, and J. Zhang (2008), A linear decision-based approximation approach to stochastic programming, *Oper. Res.*, *56*(2), 344–357.

Dyer, M., and L. Stougie (2006), Computational complexity of stochastic programming problems, *Math. Program.*, *106*(3), 423–432.

Escudero, L. (2000), Warsyp: A robust modeling approach for water resources system planning under uncertainty, *Ann. Oper. Res., 95*, 313–339.

Goh, J., and M. Sim (2010), Distributionally robust optimization and its tractable approximations, *Oper. Res., 58*(4-Part-1), 902–917.

Goh, J., and M. Sim (2011), Robust optimization made easy with ROME, *Oper. Res., 59*(4), 973–985.

Housh, M., A. Ostfeld, and U. Shamir (2012), Optimal multiyear management of a water supply system under uncertainty: Robust counterpart approach, *Water Resour. Res., 47*, W10515, doi:10.1029/2011WR010596.

Kelman, J., J. R. Stedinger, L. A. Cooper, E. Hsu, and S.-Q. Yuan (1990), Sampling stochastic dynamic programming applied to reservoir operation, *Water Resour. Res., 26*(3), 447–454.

Koutsoyiannis, D., and A. Economou (2003), Evaluation of the parameterization-simulation-optimization approach for the control of reservoir systems, *Water Resour. Res., 39*(6), 1170, doi:10.1029/2003WR002148.

Labadie, J. W. (2004), Optimal operation of multi-reservoir systems: State-of-the-art review, *J. Water Resour. Plann. Manage., 130*(2), 93–111.

Mulvey, J. M., R. J. Vanderbei, and S. A. Zenios (1995), Robust optimization of large-scale systems, *Oper. Res., 43*(2), 264–281.

Oliveira, R., and D. P. Loucks (1997), Operating rules for multi-reservoir systems, *Water Resour. Res., 33*(4), 839–852.

Pianosi, F., X. Quach Thi, and R. Soncini-Sessa (2011), Artificial neural networks and multi-objective genetic algorithms for water resources management: An application to the Hoabinh reservoir in Vietnam, paper presented at the 18th IFAC World Congress, The International Federation of Automatic Control, Milan, Italy.

ReVelle, C., E. Joeres, and W. Kirby (1969), Linear decision rule in reservoir management and design. 1. Development of the stochastic model, *Water Resour. Res., 5*(4), 767–777.

Shumway, R. H., and D. S. Stoffer (2010), *Time Series Analysis and its Applications: With R Examples*, 3rd ed., 604 pp., Springer, N. Y.

Stedinger, J. R., B. F. Sule, and D. P. Loucks (1984), Stochastic dynamic programming models for reservoir operation optimization, *Water Resour. Res., 20*(11), 1499–1505.

Takeuchi, K. (1986), Chance-constrained model for real-time reservoir operation using drought duration curve, *Water Resour. Res., 22*(4), 551–558.

Tejada-Guibert, J. A., S. A. Johnson, and J. R. Stedinger (1995), The value of hydrologic information in stochastic dynamic programming models of a multireservoir system, *Water Resour. Res., 31*(10), 2571–2579.

Tilmant, A., D. Pinte, and Q. Goor (2008), Assessing marginal water values in multipurpose multireservoir systems via stochastic programming, *Water Resour. Res., 44*, W12431, doi:10.1029/2008WR007024.

Trezos, T., and W. W.-G. Yeh (1987), Use of stochastic dynamic programming for reservoir management, *Water Resour. Res., 23*(6), 983–996.

Ugray, Z., L. Lasdon, J. Plummer, F. Glover, J. Kelly, and R. Mart (2007), Scatter search and local NLP solvers: A multistart framework for global optimization, *Inf. J. Comput., 19*(3), 328–340.

Watkins, D. W., and D. C. McKinney (1997), Finding robust solutions to water resources problems, *J. Water Resour. Plann. Manage., 123*(1), 49–58.

World Commission on Dams (2000), *Dams and Development: A New Framework for Decision-Making*, Earthscan Publ. Ltd., London.

Yeh, W. W.-G. (1985), Reservoir management and operations models: A state-of-the-art review, *Water Resour. Res., 21*(12), 1797–1818.

Yoo, J. H. (2009), Maximization of hydropower generation through the application of a linear programming model, *J. Hydrol., 376*, 182–187.